ADSORPTION STUDY OF CARBON DIOXIDE IN 'L' SHAPED SLIT PORES AT HIGH TEMPERATURES AND PRESSUERS USING MONTE CARLO SIMULATIONS

Nithin B. Kummamuru[*], Angan Sengupta, Srikanta Dinda

Department of Chemical Engineering, Birla Institute of Technology and Science, Pilani, Hyderabad Campus, India

ABSTRACT

CO_2 capture from high operating temperatures are of special interest as it is economically appealing over low temperature CO_2 capture process in Post-combustion capture. This work contributes to the estimation of new and complementary density data for CO_2 confined in 'L' shaped carbon slit pores at high temperatures and pressures. CO_2 adsorption capacities in 'L' shaped carbon slit pores of heights 20Å, 31.6Å, 63.2Å, 94.85Å and 126.5Å at 673.15 K and 873.15 K over a pressure range of 500 kPa to 4000 kPa are predicted by Grand Canonical Monte Carlo simulations. Elementary Physical Model is employed to model CO_2 at these temperatures and pressures both in bulk and confined phase. CO_2 adsorption capacities and the unique structural properties of the confined CO_2 at all the condition mentioned above has been estimated in presence of the wall-fluid interactions and the fluid-fluid interactions. The Steele wall potential is used to model the wall-fluid interactions inside carbon-based adsorbents that have a slit shaped geometry.

Keywords: Slit pores, Carbon dioxide adsorption, GCMC simulations, Structural properties, High Temperatures

NONMENCLATURE

Abbreviations	
CO_2	Carbon Dioxide
GCMC	Grand Canonical Monte Carlo
EPM	Elementary Physical Model
CCS	Carbon Capture and Storage
LJ	Lennard-Jones
RDF	Radial Distribution Function
Symbols	
ε_{ff}	Potential well depth of fluid-fluid interaction
σ_{ff}	Collision diameter
r_{ij}	Distance between two fluid atoms
q_i^{γ} and q_j^{δ}	Effective Charges on molecules i and j
ε_0	Vacuum permittivity
ρ_s	Density of carbon atoms on the adsorbent wall
Δ	Separation distance between carbon layers in the adsorbent
ε_{sf}	Well depth of adsorbate-fluid site interaction
σ_{sf}	Effective adsorbate-fluid intermolecular diameter

1. INTRODUCTION

Carbon Capture and Storage technologies, have been developed and tested intensely since the 1970s [1] to mitigate the CO_2 emissions to the atmosphere. Many promising methods were projected by CCS in capturing CO_2 from flue gas. As on date, the most mature technology in capturing CO_2 via post-combustion capture process is the chemical absorption process using aqueous alkanolamine solutions [2]. However, this process suffers number of complicating factors such as formation of stable salts due to irreversible chemical reactions between absorbent and aggressive species, degradation of solvent causing increased rate of corrosion, and high solvent regenerative energy demand [2]. Adsorption technology is therefore, considered to be a promising alternative to chemical absorption process because of low operating and maintenance costs, large adsorption capacities, fast adsorption and desorption kinetics compared to amine based absorption and exclusively for low energy penalties in regeneration processes [3]. Although present research, are advancing in developing selective and high capacity adsorbents materials [4], lot of

research is confined to estimate the adsorption capacities of CO_2 at low temperatures and pressures despite CO_2 capture at high temperatures are economically appealing nowadays [5]. Concurrently, there is inadequate understanding in adsorption/ desorption behavior of CO_2 inside such materials at elevated temperature and pressure conditions. High-performance computations have become an effective way for understanding CO_2 capture inside various adsorbents by investigating the complex interplay between the fluid-fluid and pore-fluid interactions, which estimates the unique properties of the confined CO_2 that differ significantly from the bulk phase, depending on parameters such as pore size/geometry, and surface chemistry. The traditional simulations in Grand Canonical ensemble correctly predicts the adsorption isotherms inside porous media [6] as GC ensemble is the natural ensemble for studying any thermodynamically open systems. In the present paper, CO_2 adsorption density inside 'L' shaped carbon slit pores were predicted using GCMC simulations and the effect of temperatures and pressures on adsorption-desorption isotherms are also discussed. Further, the structure of confined CO_2 inside different pore heights are also examined.

2. SIMULATION DETAILS

All the simulations were performed at temperatures 673.15 K and 873.15 K within a pressure range of 500 kPa to 4000 kPa, which corresponds to the operating conditions of methane steam reforming process [5]. Although extensive research on CO_2 adsorption at low temperature and pressure range have been performed using GCMC simulations with different adsorption models [7] and also through experiments [4]; recent research have shown that capturing CO_2 from high operating temperatures are of special interest as it is economical over low-temperature [5]. CO_2 capture processes in post combustion process CO_2 molecule in the present work is represented by the EPM [8], having 12-6 LJ sites with charges centered at each atom. The pair interactions between CO_2 molecules is given by 12-6 LJ model as shown in equation 1.

$$\varphi_{ff} = 4\varepsilon_{ff}\left[\left(\frac{\sigma_{ff}}{r_{ij}}\right)^{12} - \left(\frac{\sigma_{ff}}{r_{ij}}\right)^{6}\right] \tag{1}$$

The cutoff distance has been set to 10Å, as reported by Harris and Yung [8].The interactions between the charge on molecules are governed by Coulomb's law as shown in equation 2.

$$\Psi_{ij} = \frac{1}{4\pi\varepsilon_0}\frac{q_i^\gamma q_j^\delta}{r_{ij}^{(\gamma,\delta)}} \tag{2}$$

The partial charges on C and O atoms of CO_2 molecules are +0.6645e and -0.3322e, respectively [8]. Steele wall potential [9] (equation 3) is used to represent the walls of the slit pores (carbon based materials) in z direction (Fig 1). The ρ_s is 0.114 Å^{-3} and Δ is 3.35 Å [10].

$$\varphi_{sf} = 2\pi\varepsilon_{sf}\rho_s\sigma_{sf}^2\Delta[0.4\left(\frac{\sigma_{sf}}{z}\right)^{10} - \left(\frac{\sigma_{sf}}{z}\right)^{4} \\ - \sigma_{sf}^4/(3\Delta(z+0.61\Delta)^3)] \tag{3}$$

Lorentz-Berthelot mixing rules (equations 4 and 5) are used to represent parameters ε_{sf} and σ_{sf}.

$$\varepsilon_{sf} = \sqrt{\varepsilon_{ss}\varepsilon_{ff}} \tag{4}$$

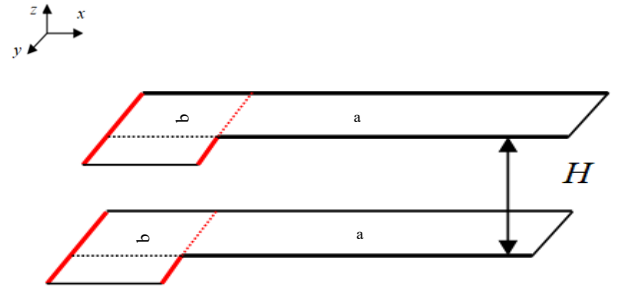$$\sigma_{sf} = \frac{\sigma_{ss}+\sigma_{ff}}{2} \tag{5}$$

Fig 1 'L' shaped slit pore divided into two slit sections a and b.

All the parameter values used for carbon dioxide and carbon based adsorbent wall are listed in Table 1. The bulk density of CO_2 at temperatures 673.15 K and 873.15 K within a pressure range of 500 kPa to 4000 kPa are predicted from the isothermal-isobaric ensemble simulations. The chemical potential values estimated via Widom Insertion technique has been further used for predicting CO_2 adsorption isotherms using GCMC simulations. The RDFs and density plots are obtained via Canonical ensemble simulations and are used to predict the attainable structure of CO_2 inside the pores. Monte Carlo simulation, for bulk phase CO_2 are initially equilibrated over 2.5 x 10^7 cycles and the property averages are considered from next 2.5 x 10^7 production cycles. Similarly, 2.5 x 10^7 equilibration cycles and 2.5 x 10^7 production cycles are performed in both the GC ensemble and the Canonical ensemble for the MC simulations inside pores of carbon-based adsorbents. In the present work CO_2 adsorption is carried out in carbon based materials having pore height (H) between 6.324σ_{sf} to 40σ_{sf} (H = 20Å to 126.5Å) with constant

pore surface area of $31.62\,\sigma_{sf}$ x $22.13\,\sigma_{sf}$. All the simulations in this work has been carried out using the open software package of MCCCS-Towhee [11].

Table 1. Molecular parameters used for CO_2 molecules and slit carbon graphite wall.

CO_2	
$\sigma_{ff}/Å$	$k_B^{-1} \cdot \varepsilon_{ff}/K$
σ_{c-c} = 2.785	$k_B^{-1} \cdot \varepsilon_{c-c}$ = 28.99
σ_{c-o} = 2.921	$k_B^{-1} \cdot \varepsilon_{c-o}$ = 49.06
σ_{o-o} = 3.064	$k_B^{-1} \cdot \varepsilon_{o-o}$ = 82.997
Graphite wall	
$\sigma_{ss}/Å$	$k_B^{-1} \cdot \varepsilon_{ff}/K$
σ_{c-c} = 3.4	$k_B^{-1} \cdot \varepsilon_{c-c}$ = 28
Mixing rule parameters	
$\sigma_{sf}/Å$	$k_B^{-1} \cdot \varepsilon_{sf}/K$
σ_{c-c} = 3.0925	$k_B^{-1} \cdot \varepsilon_{c-c}$ = 28.495
σ_{c-o} = 3.232	$k_B^{-1} \cdot \varepsilon_{c-o}$ = 48.207
$\sigma_{o-(c-o)}$ = 3.160	$k_B^{-1} \cdot \varepsilon_{c-(c-o)}$ = 37.063

3. RESULTS

This section reports the simulated adsorbed CO_2 densities and the attainable structure of CO_2 in the 'L' shaped slit pores.

3.1 CO_2 inside 'L' shaped slit pores

Fig 2 and Fig 3 shows the adsorption-desorption densities of CO_2 inside 'L' shaped carbon slit pores obtained via GCMC simulations at 673.15 K and 873.15 K, respectively at different pressures and pore heights of H = 20Å, 31.6Å, 63.2Å, 94.85Å, and 126.5Å. The estimated bulk phase CO_2 densities were simulated using isothermal-isobaric ensemble at 673.15 K and 873.15 K over a pressure range of 500 kPa to 4000 kPa. As can be seen from Fig 2 and 3 the simulated bulk densities shows an excellent agreement with the experimental densities that are reported in literature [12]. It is also noted from Fig 2 and 3 that the adsorbed CO_2 densities inside the pores show an expected increase with an increase in pressure and an expected decreases with increase in the temperature. Interestingly the adsorbed densities have decreased to 42.56% and 27.24% from an increase in pore height from 20Å to 126.5Å under highest pressure (4000 kPa) at 673.15 K and 873.15 K, respectively. As can be seen the adsorbed CO_2 densities at both the temperatures

has no significant difference inside larger pores of height 94.85Å and 126.5Å. Thus, it can now be speculated that further increase in the pore height might not show any considerable change in the CO_2 adsorbed densities. Previously reported study [13] on CO_2 adsorption inside carbon slit pore (two horizontal plates) using GCMC technique showed abrupt vapor to liquid phase change inside a pore height of 54.3Å between 2800 kPa and 3000 kPa at 298 K, however, in the present study desorption isotherms follow the adsorption isotherms and no hysteresis was observed inside the pores under these high temperatures conditions.
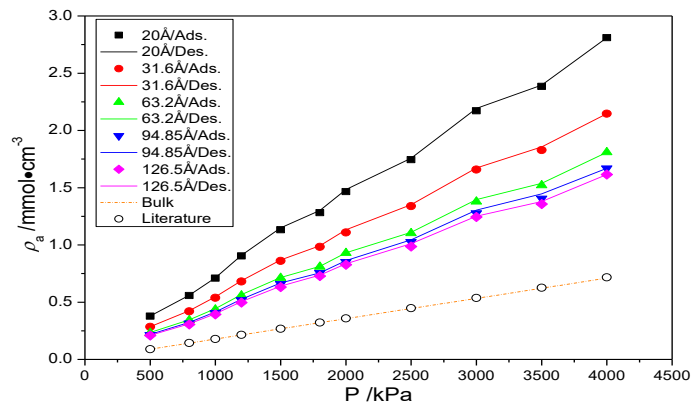

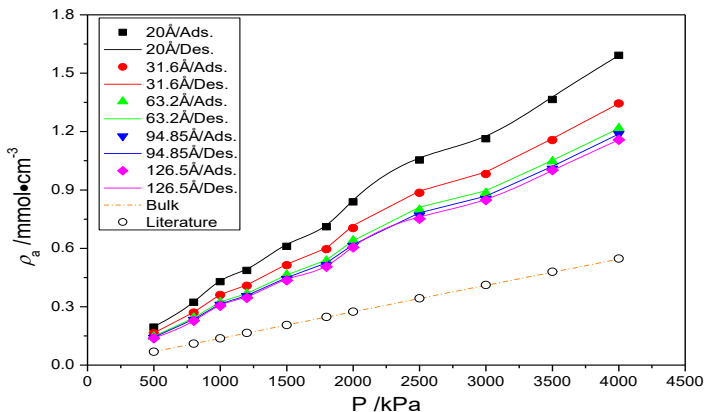Fig 2 Simulated adsorption isotherms of CO_2 in 'L' shaped carbon slit pores at 673.15 K

Fig 3 Simulated adsorption isotherms of CO_2 in 'L' shaped carbon slit pores at 873.15 K

The RDFs ($g_{xy}(r)$), where x and y are the two atoms in CO_2 molecule separated by a distance r) have also been estimated for understanding the attainable structure for CO_2 confined inside the 'L' shaped carbon slit pores of heights 20Å, 63.2Å and 126.5Å at 673.15 K and 873.15 K for pressure range of 500 kPa and 4000 kPa. As noted from Fig 4 to 7, the height of the peaks for $g_{cc}(r)$, $g_{co}(r)$, and $g_{oo}(r)$ increased with an increase in pore height from 20Å to 126.5Å. It is noted that the first
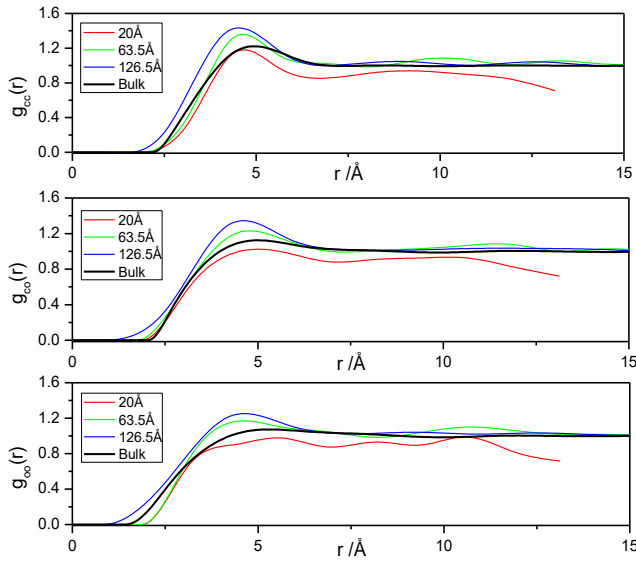
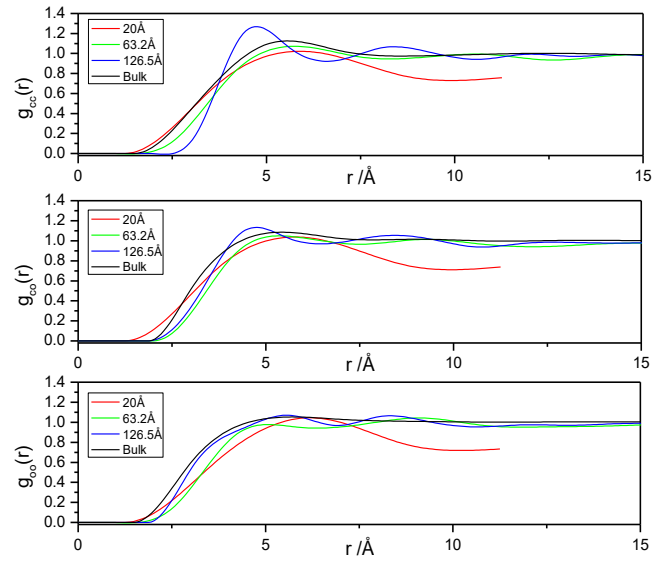Fig 4 RDFs of CO$_2$ molecules in 'L' shaped carbon slit pores and bulk phase at 500 kPa and 673.15 K

Fig 6 RDFs of CO$_2$ molecules in 'L' shaped carbon slit pores and bulk phase at 500 kPa and 873.15 K
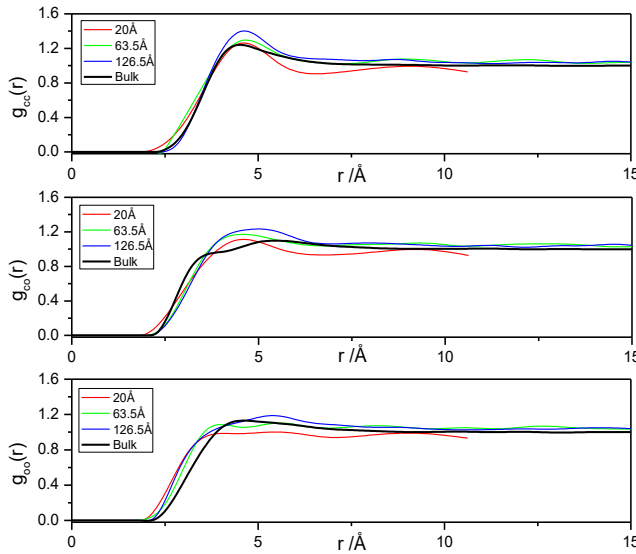

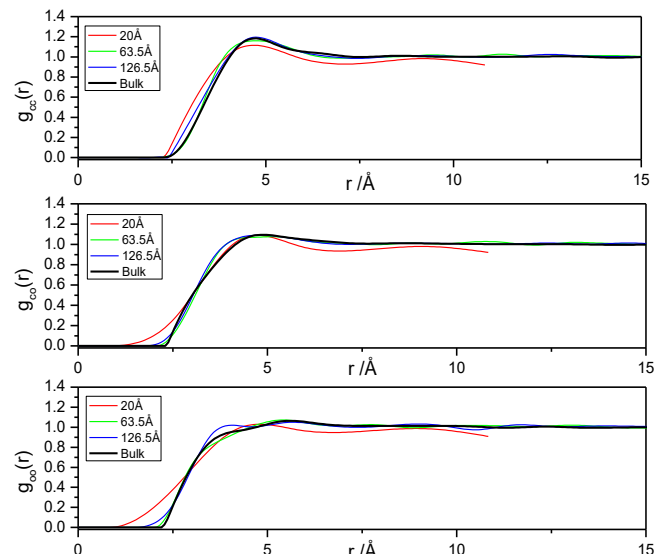Fig 5 RDFs of CO$_2$ molecules in 'L' shaped carbon slit pores and bulk phase at 4000 kPa and 673.15 K

Fig 7. RDFs of CO$_2$ molecules in 'L' shaped carbon slit pores and bulk phase at 4000 kPa and 873.15 K

peak of $g_{cc}(r)$ for all the plotted pressures and pores heights at 673.15 K and 873.15 K has been observed at 4.75Å, which is the favorable neighbor-neighbor distance between the atoms and these peaks also corresponds to the respective bulk phase C-C RDFs. However, for 20Å to 126.5Å, after the first peak, the subsequent coordination shells were also observed for all the pressures, implying liquid-like phase inside the Slit pores. Similar trend was also observed in the corresponding $g_{co}(r)$, and $g_{oo}(r)$ plots. Moreover, increase in temperature from 673.15 K to 873.15 K at constant pressure showed decrease in the peak heights for all the RDFs inferring weaker interactions between the fluid atoms at higher temperatures. Likewise a

further increase in the pore height might also show RDFs coinciding the bulk phase RDF values. Besides, the RDFs, local CO$_2$ density profiles inside the 'L' shaped carbon slit pores are also obtained for a better insight into the attainable structure of confined CO$_2$. Fig 8 to 11 shows the density profiles of CO$_2$ confined inside the 'L' shaped carbon slit pores of heights 20Å and 63.2Å at different operating conditions. The density profiles are plotted by dividing the 'L' shaped carbon slit pores into two slit parts (black and red) having surface area of 100Å x 70Å (a) and 83.67Å x 153.67Å (b) respectively as shown in Fig 1.

From Fig 8 to 11, it is observed that CO$_2$ molecules undergo layering inside the 'L' shaped carbon slit pores
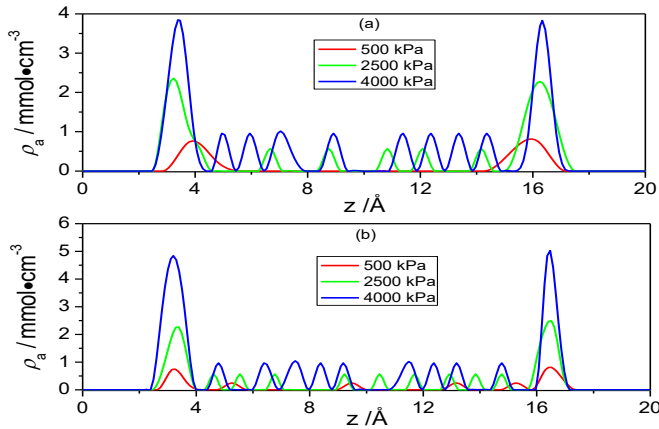
Fig 8 1D local CO_2 density profile along z direction in slit pore a and b of 'L' shaped carbon slit pore of height 20Å at 673.15 K. (a) and (b) represents density profile in section 'a' and 'b' of 'L' shaped carbon slit pore respectively.

Fig 9 1D local CO_2 density profile along z direction in slit pore a and b of 'L' shaped carbon slit pore of height 20Å at 873.15 K. (a) and (b) represents density profile in section 'a' and 'b' of 'L' shaped carbon slit pore respectively.
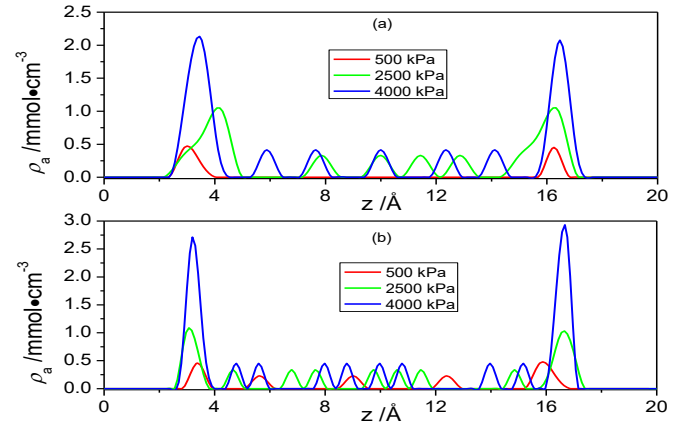

Fig 10 1D local CO_2 density profile along z direction in slit pore a and b of 'L' shaped carbon slit pore of height 63.2Å at 673.15 K. (a) and (b) represents density profile in section 'a' and 'b' of 'L' shaped carbon slit pore respectively.

at all pressure and temperature conditions indicating liquid-like phase behavior inside all the pore heights studied in this work. However, a substantial amount of CO_2 adsorption was observed near the pore walls in all the Fig (8 to 11, represented by higher peaks near the walls followed by lower peaks at the centre of the pore) due to interplay between fluid-fluid and pore-fluid interactions. As can be seen from Fig 8 to 11, the section 'b' of the 'L' shaped carbon slit pores showed more layering and higher peak heights due to greater CO_2 adsorption at respective temperatures and pressures, which is because of greater surface area compared to section 'a' of the 'L' shaped carbon slit pore. Furthermore, increasing the pressure from 500 kPa to 4000 kPa increases the number of layers inside the pores along with peak heights of the density profiles implying more adsorption in the form of liquid-like phase. Besides the effect of pressure, increase in temperature from 673.15 K to 873.15 K at a given pressure decreases the peaks heights and layer formation indicating intuitive lower adsorption at higher temperature. Also, with an increase in pore height from 20Å to 63.2Å at a given temperature and pressure the effective height of the density profile peaks decrease indicating lower densities inside larger pores, which support the observations from the isotherms (Fig 2 and 3); where increasing pore height results pore densities to shift closer to the corresponding bulk phase density values. Similar decreasing trends are observed while increasing the pore heights to 126.5Å. However, the adsorbed densities are still in liquid-like phase as more number of layers are observed at higher pores. Previously reported simulation study [13] on CO_2 adsorption in carbon slit pore of height 54.3Å showed
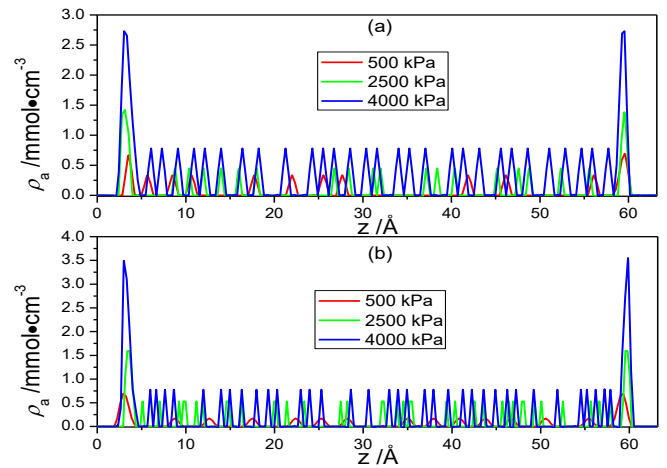
adsorption capacities of 1.6610 mmol/cm^3 and 21.5800 mmol/cm^3 at 298 K over the pressures of 500 kPa and 4000 kPa, respectively. In the present case of the 'L' shaped pores, increase in the pore-fluid interactions though results in higher adsorption compared to the parallel slit pores; however, the effect of high temperature on reduced adsorption capacity is also clearly evident from Fig 2 and 3. The present study, therefore, shows the possibility of achieving higher CO_2 adsorption capacities by increasing the slit pore surface area (thus increasing the pore-fluid interactions), pore geometry and loading pressures at higher operating temperatures which might economically benefit the post combustion CO_2 capture technology.

4. CONCLUSION

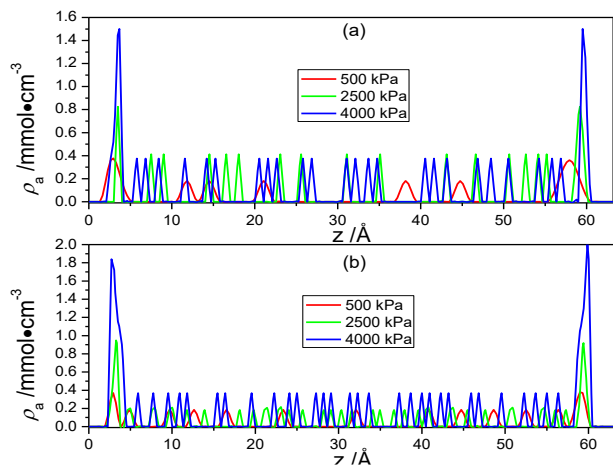The new and complementary density data for CO_2

Fig 11 1D local CO_2 density profile along z direction in slit pore a and b of 'L' shaped carbon slit pore of height 63.2Å at 873.15 K. (a) and (b) represents density profile in section 'a' and 'b' of 'L' shaped carbon slit pore respectively.

confined in 'L' shaped carbon slit pores at high temperatures and pressures are estimated via GCMC simulations and represented in the present paper. CO_2 in both bulk phase and in the 'L' shaped carbon slit pores has been modeled using EPM at temperatures 673.15 K and 873.15 K for pressures from 500 kPa to 4000 kPa, which corresponds to the operating condition of methane steam reformation process. The estimated bulk phase densities obtained from isothermal-isobaric ensemble simulations showed good agreement with the literature values. The CO_2 adsorption capacity inside 'L' shaped carbon slit pores (modeled using Steele wall potential) for the pore heights ranging from 20Å to 126.5Å showed an increase with increase in pressures and decrease with an increase in temperature. Also the, increase in pore heights resulted in a decrease in the adsorbed densities. Consequently, at higher slit pores of heights 94.85Å and 126.5Å no significant difference in adsorbed densities are observed. Moreover, the RDFs with subsequent coordination shells in all the pores indicated liquid-like behavior, albeit lesser peak heights at higher temperatures. In addition to RDFs, the density plots inside the 'L' shaped slit pores also revealed the structure of adsorbed layers. An increase in operating pressures showed more layering inside the pores indicating more adsorption and attainment of liquid-like phase. It is interesting to note that inside the 'L' shaped slit pore though the adsorption capacity decreases with the increase in slit height, the adsorbed phase behaves more like liquid-phase (with more number of layers and increased peak heights in the density profiles) at a temperature greater than the critical temperature (T_c) of CO_2 (304.12 K [14]).

REFERENCE

[1] Kohl A, Nielsen R. Gas Purification. Houston: Gulf Professional Publishing; 1997.
[2] Wu X, Yu Y, Qin Z, Zhang Z. The advances of post-combustion CO_2 capture with chemical solvents: review and guidelines. Energy Procedia 2014; 63:1339-1346.
[3] Songolzadeh M, Ravanchi M, Soleimani R. Carbon Dioxide Capture and Storage: A General Review on Adsorbents. World. Acad. Sci. Eng. Technol. 2013; 6:225-232.
[4] Amanda A, Moral-Vico J, Markeb A, Busquets-Fite M, Komilis. D, Puntes V, *et al.* Critical review of existing nanomaterial adsorbents to capture carbon dioxide and methane. Sci. Total. Environ 2017; 595:51-62.
[5] Seggiani M, Puccini M, Vitolo S. Alkali promoted lithium orthosilicate for CO_2 capture at high temperature and low concentration. INT. J. GREENH. GAS. CONT. 2013; 17:25-31.
[6] Balbuena P, Gubbins K. Classification of adsorption behavior: simple fluids in pores of slit-shaped geometry. Fluid. Phase. Equilibr 1992; 76:21-35.
[7] Hedin N, Chen L, Laaksonen A. Sorbents for CO_2 capture from flue gas—aspects from materials and theoretical chemistry. Nanoscale 2010; 2:1819-1841.
[8] Harris J, Yung K. Carbon Dioxide's Liquid-Vapor Coexistence Curve and Critical Properties As Predicted by a Simple Molecular Model. J. Phys. Chem. 1995; 99:12021-12024.
[9] Steele W. The physical interaction of gases with crystalline solids. Surf. Sci. 1973; 36:317-352.
[10] Lastoskie C, Gubbins K, Quirke N. Pore size heterogeneity and the carbon slit pore: A density functional theory model. Langmuir 1993; 9:2693-2702.
[11] Martin M. MCCCS Towhee: a tool for Monte Carlo molecular simulation. Mol. Simulat 2013; 39:1212-1222.
[12] Span R, Wagner W. A New Equation of State for Carbon Dioxide Covering the Fluid Region from the Triple-Point Temperature to 1100 K at Pressures up to 800 MPa. J. Phys. Chem. Ref. Data. 1996; 25:1509-1596.
[13] Lithoxoos G, Peristeras L, Boulougouris G, Economou I, Monte Carlo simulation of carbon monoxide, carbon dioxide and methane adsorption on activated carbon. Mol. Phys. 2012; 110:1153-1160.
[14] Moldover M. Visual observation of the critical temperature and density: CO_2 and C_2H_4. J. Chem. Phys. 1974; 61:1766-1778.